IARJSET

ISSN (Online) 2393-8021
ISSN (Print) 2394-1588

International Advanced Research Journal in Science, Engineering and Technology

ISO 3297:2007 Certified

Vol. 4, Issue 12, December 2017

Analysis of Warm Forming of Locally Heated Sheet Metals by Using Finite Element Analysis

Mahmut TANDOGAN[1], Omer EYERCIOGLU[2]

Research Assistant, Department of Mechanical Engineering, Gaziantep University, Gaziantep, 27310, Turkey[1]

Professor Doctor, Department of Mechanical Engineering, Gaziantep University, Gaziantep, 27310, Turkey[2]

Abstract: Automotive industry uses stainless steels for place where needed corrosion resistance and magnesium alloys to reduce weight of chassis. High mechanical properties of these materials are reasons for preference however low formability of these materials in the ambient temperature creates manufacturing problems. In this study, enhancement of bending ability of a stainless steel and a magnesium alloy by local heating was investigated. The specimens were bent in V-bending die by using a servo-press at room temperature. Load and deformation rate were determined during forming process. Final shapes were measured by Coordinate Measuring Machine (CMM). Same procedures were conducted with locally heating (heating the region of deformation) and the results were compared with cold forming. It was observed that locally heating the bending area was adequate to give form the workpiece and this result was verified with finite element modelling.

Keywords: Locally Heating, Formability, Stainless Steel, Magnesium Alloy, Finite Element Modelling.

I. INTRODUCTION

In automobiles, there are some applications where the chassis is completely produced from stainless steels. Since corrosion resistance remains fundamental requirement for these applications, selection of grades and stabilizing elements are critical for such applications and depend primarily on operating conditions. Stainless steels are also being used in other applications such as fuel tank, mudguard, chassis for buses and trucks. With the development of new varieties of austenitic, ferritic and martensitic stainless steels, automotive industry is intensively exploring their potential [1].

Applications of magnesium in the automotive industry can significantly contribute to greater fuel economy. The usage of magnesium in automotive applications is also assessed for the impact on environmental conservation. Recent developments in coating and alloying of Mg improved the creep and corrosion resistance properties of magnesium alloys for elevated temperature and corrosive environments [2].

Eun-Ho Lee et al. [3] exhibit advantages of locally heating on springback of non-quenchable advanced high-strength steels. In the mentioned study Near-Infrared Ray (NIR) method was used for local heating the specimens. Special devices were designed to obtain regular heating on the specimen. These devices lead heating energy on the specimen bending area. Specimens were locally and completely heated up to different temperatures (20^0C, 200^0C, 400^0C, 600^0C and 700^0C). Hardness, springback and microstructural changing of specimens were compared for locally and completely heating conditions. Hıno et al. [4] studied on a new incremental sheet metal forming method and aimed to shape difficult to form materials (A5083 and AZ31). In this method, workpiece was held between blank holders and die rotated counter-clockwise and then rotated clockwise. Punch has built-in heating unit and moves perpendicular to workpiece surface. During formation operation temperature of workpiece was increased up to 875 K. This gradually turning and translating movement continues until final shape was obtained. By forming, 15^o and 25^o cone angles were achieved for A5083 and AZ31 materials with this method. Kim et al. [5] compared formability of locally heated AZ31 circular sheet by using Erichsen test with a different temperature and strain rate values and took into account fracture failure criteria (N.Cockroft, Brozzo and Ayada). Experimental and theoretical results were overlapped with Cockroft-Latham criteria.

Tokita et al. [6] studied on stretch formability of high strength steels at warm temperature. Galvanized and annealed steels have been formed by spherical stretch forming test apparatus at different temperatures between room temperature and 600°C. Initial experiments showed that in warm forming maximum formable dome height without cracks is lower than cold forming even though, material strength reduces at elevated temperature. Reason of this poor stretch formability is explained with surface temperature and strain in spherical stretch forming test apparatus. Ebrahimi et al. [7] studied on microstructure of magnesium alloy (AZ91) at high temperatures. Hot compression test was conducted at a temperature changing from 350°C and 425°C and at strain rate from $0.1s^{-1}$ to $0.5s^{-1}$. It is observed that entire conducted temperatures, by increasing strain, the number of recrystallized grains first increases and they reaches a maximum value and then decreases. The change in microstructure of magnesium alloy was observed using Scanning Electron Microscope (SEM) and Optical Microscope (OM). Al-Zubaydi et al. [8] investigated superplastic behaviour of AZ91. For this reason one disk which has 0.6 mm thickness and 10 mm diameter was placed into High Pressure Torsion

IARJSET
ISSN (Online) 2393-8021
ISSN (Print) 2394-1588
International Advanced Research Journal in Science, Engineering and Technology
ISO 3297:2007 Certified
Vol. 4, Issue 12, December 2017

(HPT) test apparatus and test was conducted at room temperature, at speed of 1 rpm using applied pressure of 3 GPa for differing number of turns (1, 3, 5, 10 turns). Miniature tensile test sample (1 mm x 0.9 mm x 0.6 mm) was cut from the disk to operate tensile test. Tensile tests were conducted at different strain rates and temperatures; the highest value of elongation was observed 1308% for 573 K and $10^{-4}\ s^{-1}$. Kim et al.[15] (2010) investigated failure of AZ31 under consideration of different process parameters (temperature and strain rate values) which has been incorporated based on developed linear correlation and three different ductile criterias Cockroft-Latham, Normalized Cockroft-Latham and Freudenthal.

In this study, numerical modelling and experimental investigation of locally warm forming of AZ91B magnesium alloy and 1.4003 stainless steel with linear bending die movement were carried out. For this purpose sheet metal bending specimens are modelled by using finite element method and warm forming analyses are done. The experimental studies are carried out to determine boundary conditions of finite element analyses.

II. Experimental Study and Finite Element Modelling

A. Workpiece Materials

In this study, AZ91B magnesium alloy and 1.4003 stainless steel have been used as workpiece materials. Both of these materials are purposely selected as they are difficult to form. AZ91B magnesium alloy is very sensitive to temperature and generally worked out at elevated temperatures. Therefore, the feasibility of forming by local heating is studied.

Magnesium is one of the most abundant metal elements in the earth. The most important characteristic of magnesium is its low density, 1.74 g/cm3. Magnesium has a higher specific strength and stiffness than many other engineering materials, including aluminium, steel and polymer-based composites [6]. Chemical composition and mechanical property of AZ91B are given in Table 1 and Table 2.

TABLE 1. Chemical Composition of AZ91B (in mass base) [7]

Aluminium, Al	Zinc, Zn	Copper, Cu	Manganese, Mn	Magnesium, Mg
9 %	0.7 %	0.3 %	0.13 %	Remainder

TABLE 2. Mechanical Properties of AZ91B [7]

Tensile strength	Yield strength	Poisson's ratio	Elastic modulus	Elongation
230 MPa	150 MPa	0.35	44.8 GPa	3 %

1.4003 stainless steel is designated according to EN10027-2 which indicates chemical composition. The first number, refers to the general structural steel with specified tensile strength is less than 500 MPa. The second number refers to the stainless and heat resisting steels. The third number indicates stainless steel with Nickel < 2.5 % without Molybdenum, Niobium and Titanium. Last two numbers refers to sequence number for stainless steels as shown in Fig.1. 1.4003 is named according to European standard, it also designated as 3Cr12, S40977, X2CrNi12 by AISI (American Iron and Steel Institute), UNS (Unified Numbering System) and DIN (Deutsches Institut für Normung) respectively.

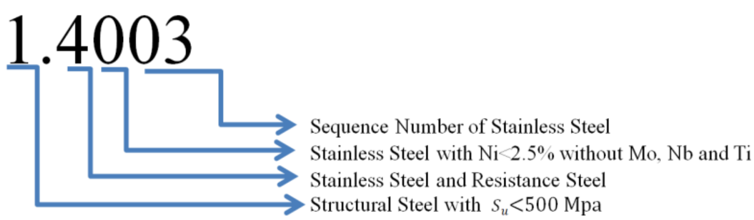

Fig. 1 Designation of 1.4003 Stainless Steel

The mechanical properties and the chemical composition of the 1.4003 stainless steel which is used in this study are determined by using tensile test and spectro-analysis, respectively. The stress-strain curve obtained from the tensile test is shown in Fig. 2 and the chemical composition is given in Table 3. Both of these results are in agreement with the certificate of 1.4003.

IARJSET
ISSN (Online) 2393-8021
ISSN (Print) 2394-1588
International Advanced Research Journal in Science, Engineering and Technology
ISO 3297:2007 Certified
Vol. 4, Issue 12, December 2017

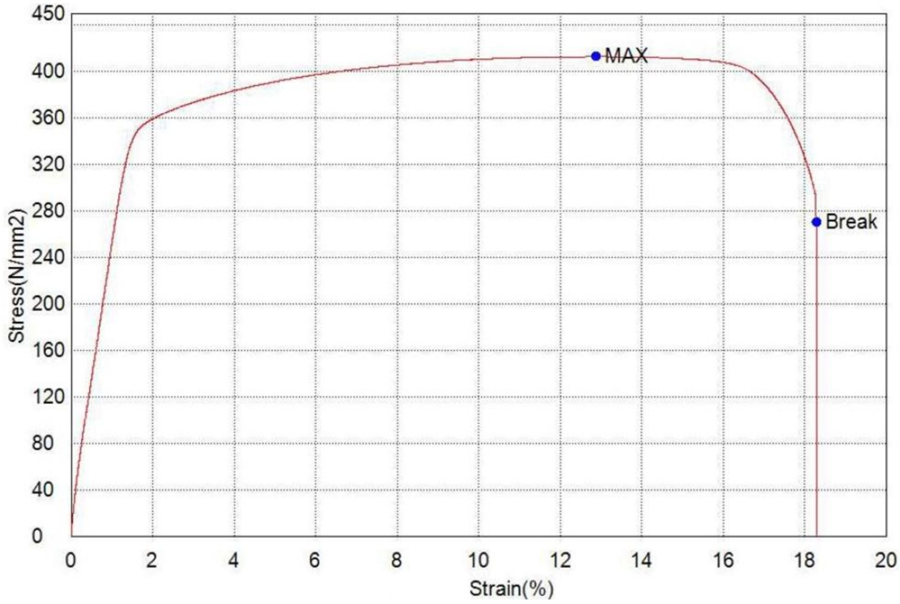

Fig. 2 Stress-Strain Graph of Specimen (1.4003)

TABLE 3 Chemical Composition of 1.4003 Stainless Steel

C	Cr	Mn	Si	P	S	Ni	N	Fe
0-0.03%	10.5-12.5%	0-1.5%	0-1%	0-0.04%	0-0.2%	0.3-1%	0-0.03%	Balance

B. Experimental Procedure

In this study V- bending die was used for experimental work. The photograph and the schematically representation of the V-bending die are illustrated in Fig. 3 and Fig. 4, respectively.

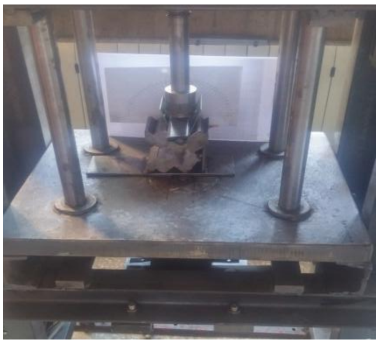
Fig. 3 Die Set

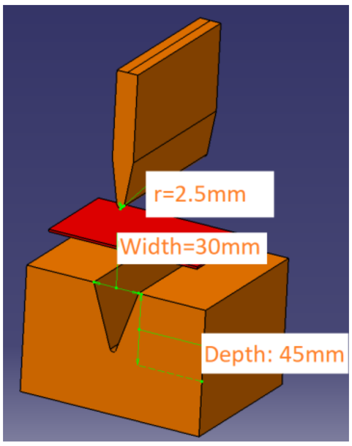

Fig. 4 Illustration of V-Bending

 DOI 10.17148/IARJSET.2017.41208

IARJSET
ISSN (Online) 2393-8021
ISSN (Print) 2394-1588
International Advanced Research Journal in Science, Engineering and Technology
ISO 3297:2007 Certified
Vol. 4, Issue 12, December 2017

Ease of manufacture and observability of degree of bending are some of the reasons why V-bending is used. In this study bending tests were conducted by using servo controlled press machine. The press has maximum capacity of 2000 kg. The loads were measured by using load cell of type Keli LFSC-A 50 kN capacity. Punch pressed the specimens with a rate of 10 mm/sec via servo press. To obtain desired angles, required stroke values were input to servo press control unit.

C. Specimen Preparation and Heating

Firstly AZ91B specimens were cut as rectangular dimension (60 mm x 170 mm x 1.5 mm). The specimens were bent with different bend angles (60° , 75° and 90°) at 10 mm/sec by the servo press. The specimens were heated up to 180℃ by resistance heating. Level of temperature was measured by infrared heat measurement device during heating process. Heated specimens was placed onto die and bent at 150℃. Changing colour of film layer was observed because of heating. The 5 mm thick specimens cut from 1.4003 stainless steel sheet plate. The specimens cut to required dimension (60 mm x 100 mm x 5 mm) by laser cutting machine. Workpiece were placed into V-bending die and pressed. The specimens were heated up to 570℃. During bending operation due to slipping grain heat occurs, this heat increases temperature up to 600℃. The reason of choosing the 600℃ for forming temperature is the reduction of yield strength at this temperature (see Fig. 5)

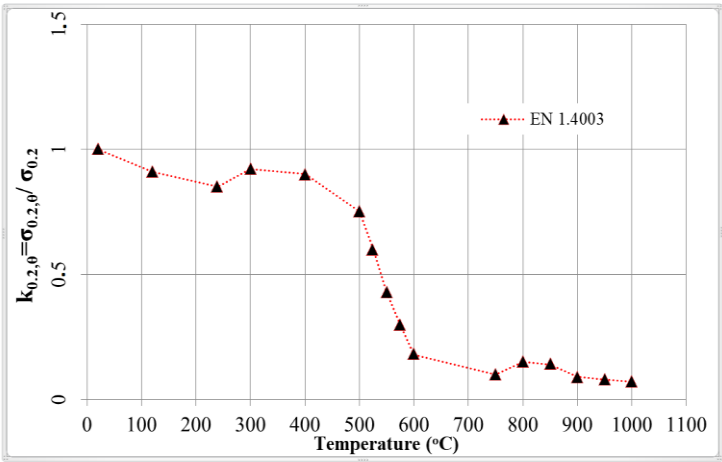

Fig. 5 Changing Yield Strength of 1.4003 Stainless Steel with respect to Temperature [9]

D. Finite Element Modelling

In this study, upper die and bottom die were taken as rigid bodies and the workpiece was defined as elastoplastic material. The rigid-elastoplastic modelling reduces simulation time by defining interface contact elements easily. This is a general route in Deform^{TM} 2D for metal forming problems. If tool stresses are needed, a subsequent run must be carried out by transferring interface loads on die components. Owing to providing realistic results in terms of springback and thermal property, workpiece materials were selected as elastoplastic material type. Mechanical properties of AZ91B and 1.4003 were not available in Deform^{TM} 2D default database, so required mechanical properties for this study was input the database. Flow stress-strain curves for AZ91B and 1.4003 was shown in Fig. 6 and 7.

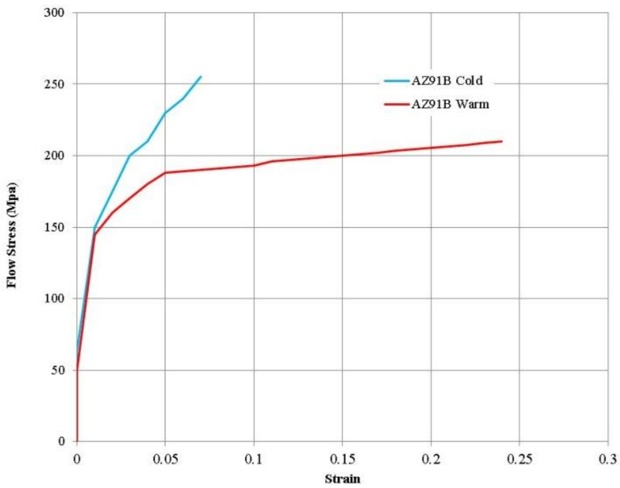

Fig. 6 Flow Stress - Strain Curves for AZ91B Cold (25^{0}C) and Warm (150^{0}C) for 0.2 mm/min Strain Rate

IARJSET
ISSN (Online) 2393-8021
ISSN (Print) 2394-1588
International Advanced Research Journal in Science, Engineering and Technology
ISO 3297:2007 Certified
Vol. 4, Issue 12, December 2017

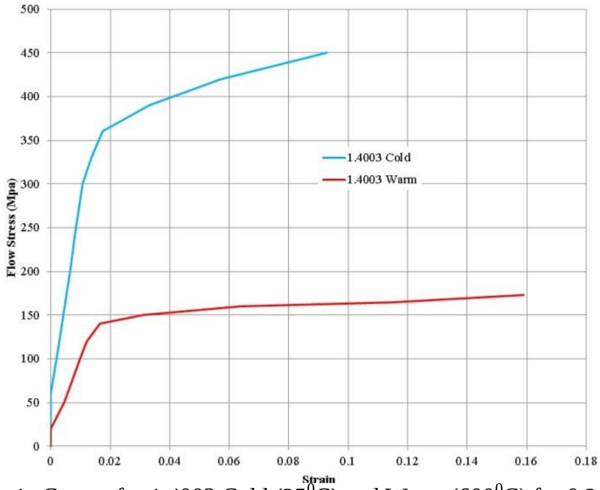

Fig. 7 Flow Stress - Strain Curves for 1.4003 Cold (25^0C) and Warm (600^0C) for 0.2 mm/min Strain Rate

Ductility of metallic materials is generally defined as the ability to deform plastically without fracture. It is usually expressed as a measure of the strain at fracture in a tension test. However the percentage elongation in a tensile test is often dominated by the uniform elongation, which is dependent on the slope of the stress-strain curve. The end of uniform elongation coincides with the onset of plastic instability. It appears that the elongation value is too complex to be regarded as a fundamental property of a material and seems reasonable to assume that any criterion of fracture will be based on some combination of stress and strain rather than on either of these quantities separately. In this study Normalized Cockroft-Latham is used as fracture criterion [10]. This fracture criterion is expressed with following formulation:

$$\int_0^{\varepsilon_f} \frac{\sigma_{max}}{\sigma_E} d\varepsilon_{pl} = C \qquad (1)$$

where

σ_{max} = The maximum principle stress $\qquad \varepsilon_f$ = The limit fracture strain
ε_{pl} = The plastic strain $\qquad \sigma_E$ = The effective stress

The critical damage factor can be obtained by using tensile test. The damage factors of AZ91B were obtained as 0.12 and 0.84 for 25°C and 150°C, respectively. The damage factors of 1.4003 stainless steel were obtained as 0.35 and 1.8 for 25°C and 600°C, respectively. Cracks begin when the damage value of workpiece reaches to its critical value. In the finite element model, the crack is shown by element deletion. Deform package can be used for axisymmetric, plane strain and torsion modelling. According to workpiece geometry this condition is selected from in simulation control window of Pre-Processor section in Fig. 8. The bending process modelled in this study is considered as plane strain problem due to high width to thickness ratio.

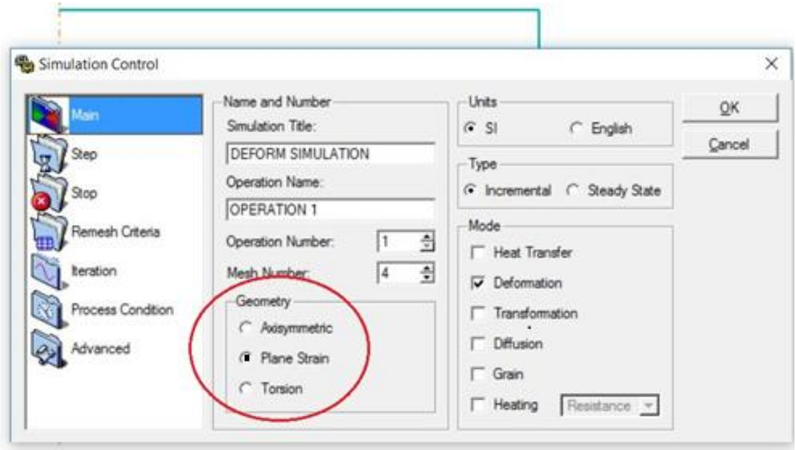

Fig. 8 Simulation Control Window

Also, friction types and values are other parameters for metal forming process. The friction values were defined between the workpiece and the bottom die, and the workpiece and the punch. The friction type was selected as Coulomb's model and the values were determined from ring compression tests. Table 4 shows the friction values for each type of models.

IARJSET
ISSN (Online) 2393-8021
ISSN (Print) 2394-1588
International Advanced Research Journal in Science, Engineering and Technology
ISO 3297:2007 Certified
Vol. 4, Issue 12, December 2017

TABLE 4 Friction Values

TYPES	AZ91B		1.4003 Stainless Steel	
	Cold	Warm	Cold	Warm
Workpiece-Bottom Die	0.14	0.33	0.12	0.3
Workpiece-Punch	0.14	0.33	0.12	0.3

Mesh and node number must be defined to any FE package. Mesh type is quadrilateral for Deform FEM software. AMG (Automatic Mesh Generator) is a tool of DEFORM and it is used to solve the problems in large deformation and to provide an optimized re-meshing capability. The Newton-Rapson Method and the Langrangian incremental type were used for iteration method and the solver, respectively. The number of elements and nodes used in the models are shown in Table 5.

TABLE 5 Elements and Nodes Numbers

TYPE	AZ91B Cold & Warm AZ91B Warm			
	Elements	Nodes	Elements	Nodes
Workpiece	2971	3430	2971	3430
	1.4003 Cold & Warm 1.4003 Warm			
	Elements	Nodes	Elements	Nodes
Workpiece	1566	1715	1566	1715

III. RESULTS AND DISCUSSION

A. Experimental and Finite Element Results for AZ91B Bending

The specimens made from AZ91B were bent for different angles (60°, *75°* and 90°) by using die described in above. The bending tests were carried out as cold and locally heated condition. Firstly cold bending was conducted up to 90° inside bending angle, as shown in Fig. 9.

Fig. 9 Cold Bent Specimens with Angle of 90°

No crack was observed at 90° cold bending, because minimum condition to cracking was not satisfied in terms of formability. Some scratches were observed on contact region of specimen and punch due to pressing. The results of FEM simulation are in well agreement with experimental one as shown in Fig. 10.

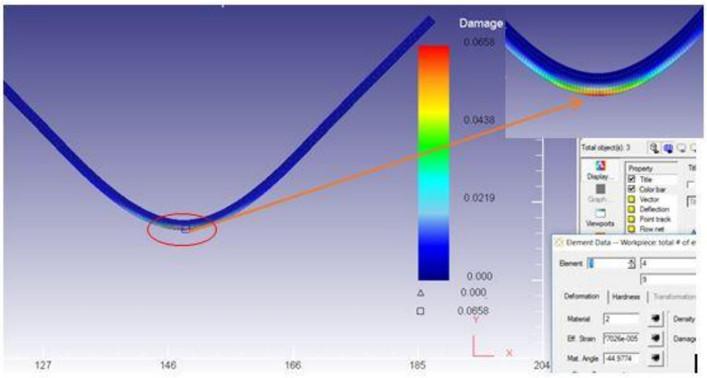

Fig. 10 Cold Bent Specimen with Angle of 90° in Deform^{TM} 2D.

IARJSET
ISSN (Online) 2393-8021
ISSN (Print) 2394-1588
International Advanced Research Journal in Science, Engineering and Technology
ISO 3297:2007 Certified
Vol. 4, Issue 12, December 2017

Secondly, cold bending was carried out with an angle of 75° which is shown in Fig. 11. Crack was not observed for this angle in experiment.

Fig. 11 Cold Bent Specimen with Angle of 75°

Fig. 12 shows the FEA for cold bent specimen with angle of 75° and damage factor did not reach to the critical value for cold forming of AZ91B.

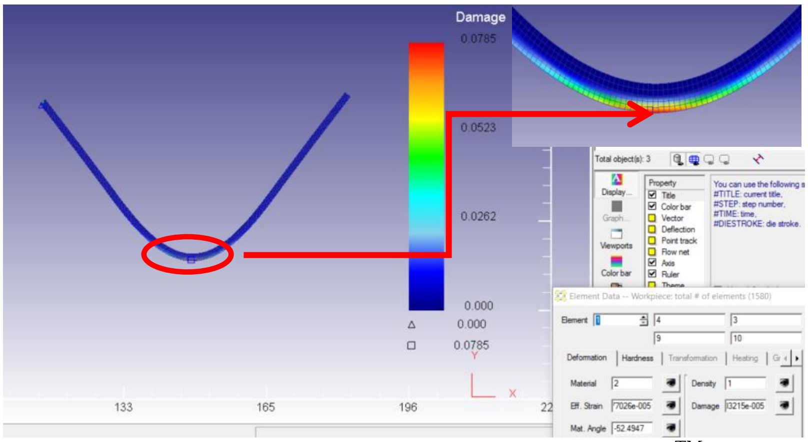

Fig. 12 Cold Bent Specimen with Angle of 75° in Deform^{TM} 2D.

Thirdly, cold bending was conducted for bend angle of 60°, as shown in Fig. 13. Cracks were observed at bend angle of 60° for cold bending process.

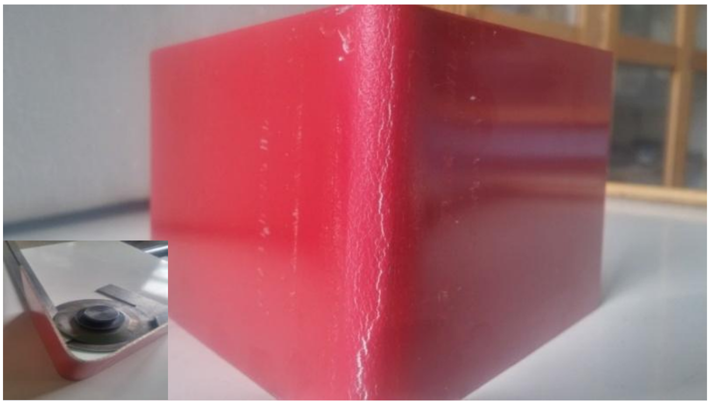

Fig. 13 Cold Bent Specimen with Angle of 60°

Finite element analysis results were in good agreement with the experimental results for this angle. The damage factor for this bending (0.124) condition was higher than the critical damage factor value (0.12). Because of this reason, cracks started which is shown in Fig. 14.

IARJSET
ISSN (Online) 2393-8021
ISSN (Print) 2394-1588
International Advanced Research Journal in Science, Engineering and Technology
ISO 3297:2007 Certified
Vol. 4, Issue 12, December 2017

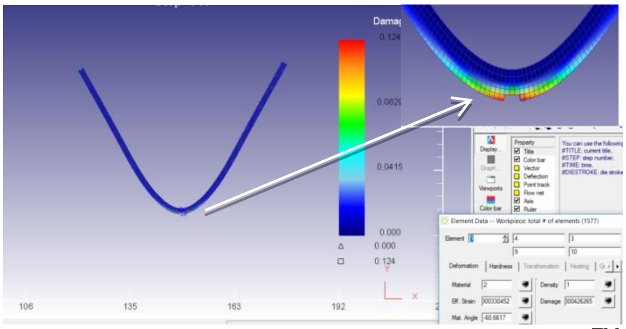

Fig. 14. Cold Bent Specimen with Angle of 60° in Deform^{TM} 2D

Summary of crack conditon of cold bending for AZ91B was shown in Table 6.

TABLE 6 Summary of Cold Bending for AZ91B

Temp.	Bend Angle	Crack for Experimental	Crack for FEM	Damage Factor in FEM
Room	90	No	No	0.065
Room	75	No	No	0.078
Room	60	Yes	Yes	0.124

Load-stroke diagram for experimental results of AZ91B was shown in Fig. 15. The load stroke diagram obtained from FE simulation was superimposed in Fig. 15. The maximum difference between load values obtained from experimental study and FEM is 9.2 %. This difference may come from friction condition.

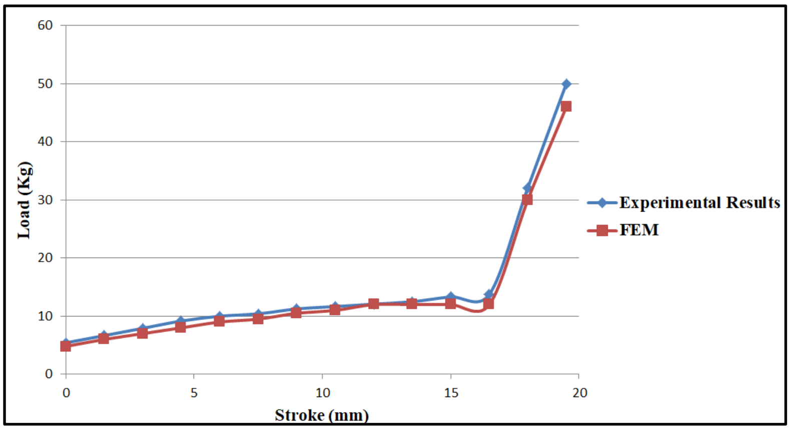

Fig. 15 Load-Stroke Diagram of Cold Bending of AZ91B

B. Experimental and Finite Element Results for AZ91B Locally Heated Bending

After cold bending process for AZ91B, specimens were locally heated and bent experimentally and FEM was simulated for locally heated specimens as shown in Fig. 16.

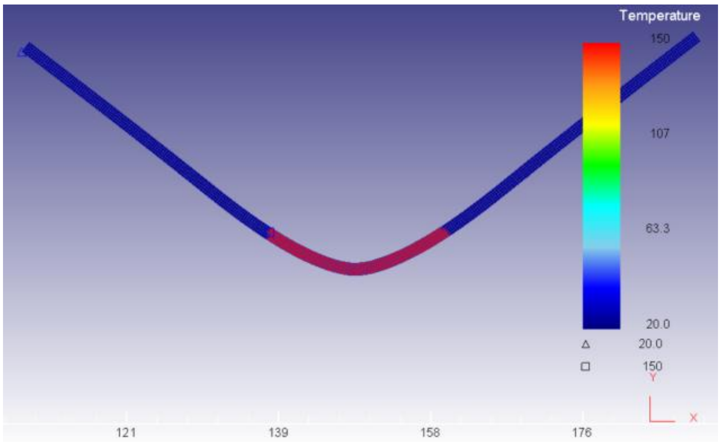

Fig. 16 Locally Heated Specimen

Firstly specimen was heated up to 180℃ by resistance heating and bent angle of 90° experimentally as shown in Fig. 17. The crack formation was not observed. Colour changing was seen because surface paint of sheet burnt out as illustrated

IARJSET
ISSN (Online) 2393-8021
ISSN (Print) 2394-1588
International Advanced Research Journal in Science, Engineering and Technology
ISO 3297:2007 Certified
Vol. 4, Issue 12, December 2017

in Fig. 18. In finite element model, damage factor did not reach the maximum, so it was in good agreement with experimental study.

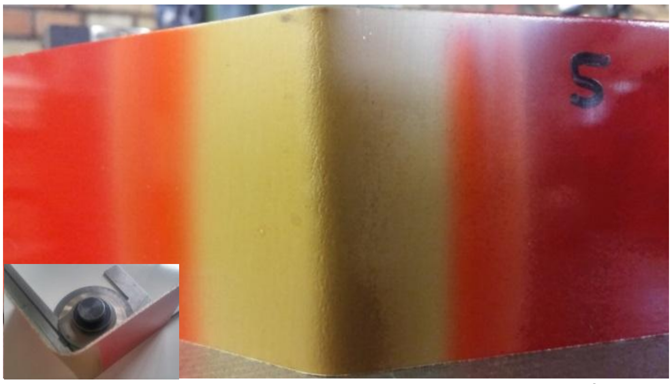

Fig. 17 Locally Heated Bent Specimen with Angle of 90°

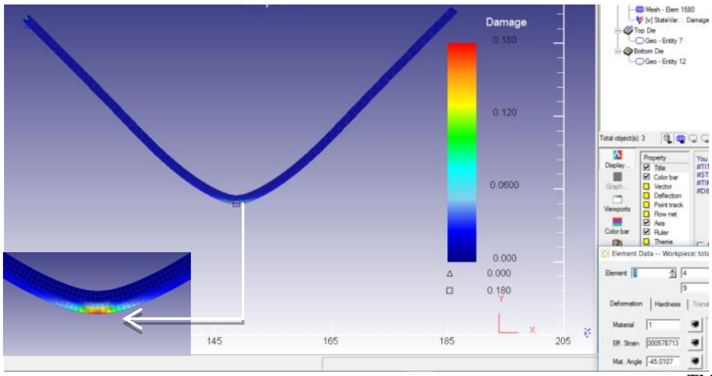

Fig. 18 Locally Heated Bent Specimen with Angle of 90° in Deform^{TM} 2D

Specimen was bent angle of 75° by using locally heating, Fig. 19 shows the still there was no crack on the outer side of bending area of specimen. This condition was in good agreement with FE results as shown in Fig. 20.

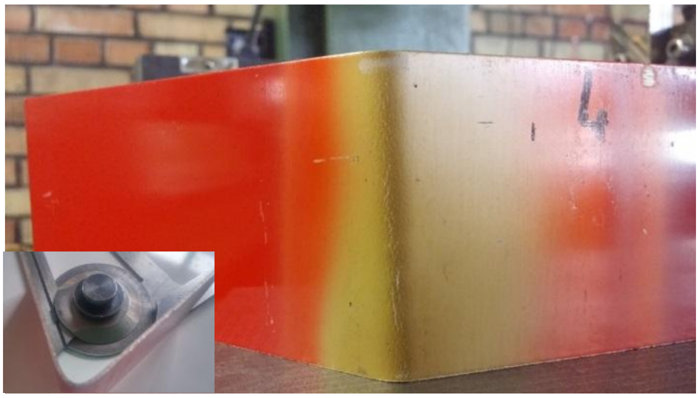

Fig. 19 Locally Heated Bent Specimen with Angle of 75°

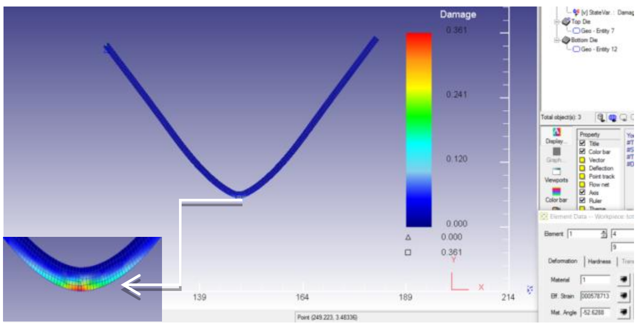

Fig. 20 Locally Heated Bent Specimen with Angle of 75° in Deform^{TM} 2D

ISSN (Online) 2393-8021
ISSN (Print) 2394-1588

Then 60° bend angle was applied the specimen as shown in Fig. 21 and Fig. 22. Crack formation was not observed, the scratch on the surface is on the surface paint.

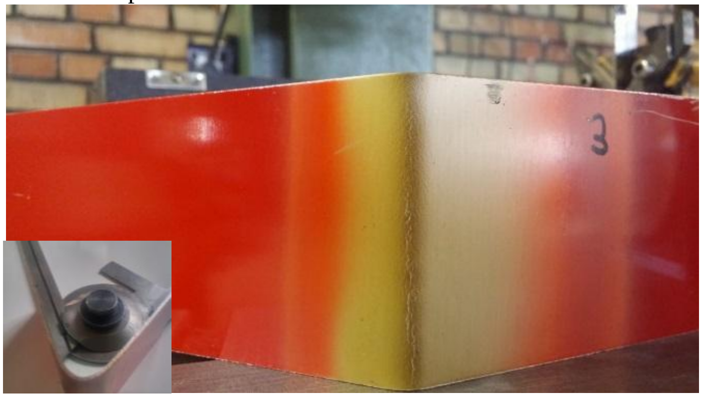

Fig. 21 Locally Heated Bent Specimen with Angle of 60°

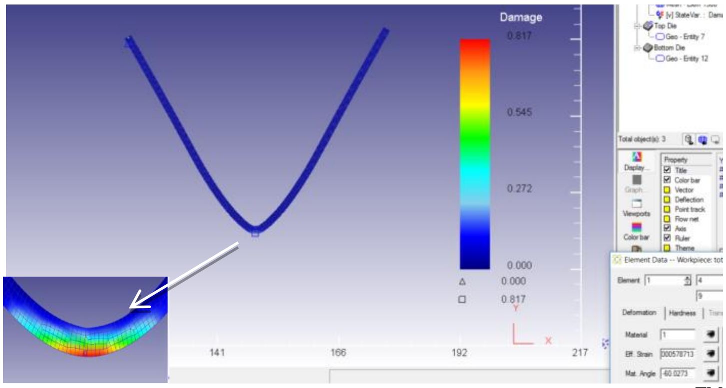

Fig. 22 Locally Heated Bent Specimen with Angle of 60° in Deform™ 2D

Load stroke diagram of locally heated AZ91B for V-bending process is shown in Fig. 23. Bending load is low and almost same until the specimen reaches to 60° bend angle. In cold forming maximum load was obtained as nearly 50 kg, however in locally heated forming this load occurred as 12 kg.

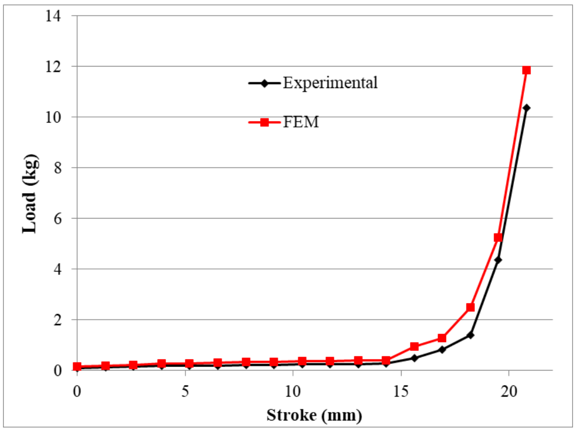

Fig. 23 Load-Stroke Diagram of Locally Heated AZ91B

C. Experimental and Finite Element Results for 1.4003 Bending

The cracks were formed on *90°* cold bending of 1.4003 stainless steel specimens. It was expected because the corresponding bend radius is lower than the minimum radius value (R_{min}). It is recommended that minimum bend radius of 1.4003 stainless steel should not be smaller than the sheet thickness [36]. The bent angle measurement of FARO Prime FaroArm coordinate measuring machine (CMM) and the photograph of the specimen are shown in Fig. 24. The bending cracks were observed at angle of 87°57′*49.11″* as shown in Fig. 25.

IARJSET
ISSN (Online) 2393-8021
ISSN (Print) 2394-1588
International Advanced Research Journal in Science, Engineering and Technology
ISO 3297:2007 Certified
Vol. 4, Issue 12, December 2017

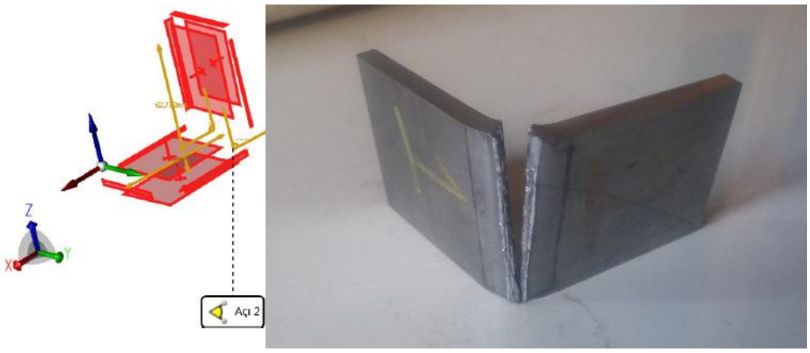

Fig. 24 Illustrations of Formed Workpieces Measured by CMM and Cold Bent Workpiece.

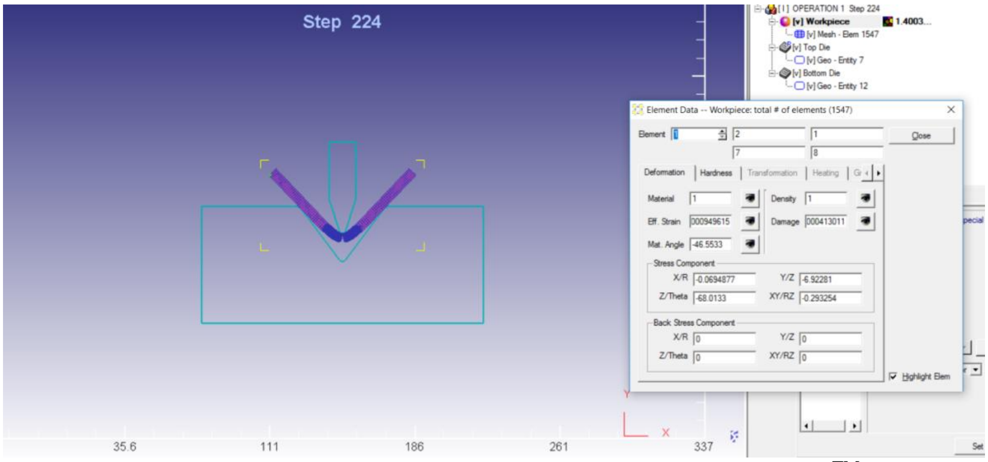

Fig. 25 Illustration of Cold Bending of 1.4003 Final Angle in Deform^{TM} 2D

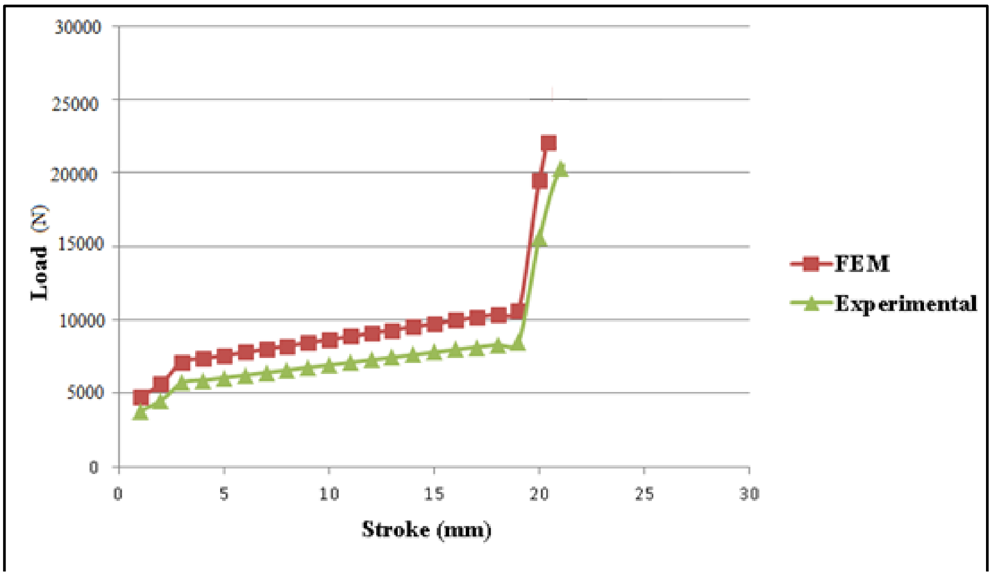

Fig. 26 Load Stroke Diagram of Cold Bending of 1.4003

The load stroke curves obtained from experimental work and FEA for cold bending of 1.4003 specimens are given in Fig. 26. As it was shown there are little differences in bending loads between experimental work and Deform^{TM} 2D simulations. The difference in load is due to lubrication (i.e. friction coefficient).

IARJSET
ISSN (Online) 2393-8021
ISSN (Print) 2394-1588
International Advanced Research Journal in Science, Engineering and Technology
ISO 3297:2007 Certified
Vol. 4, Issue 12, December 2017

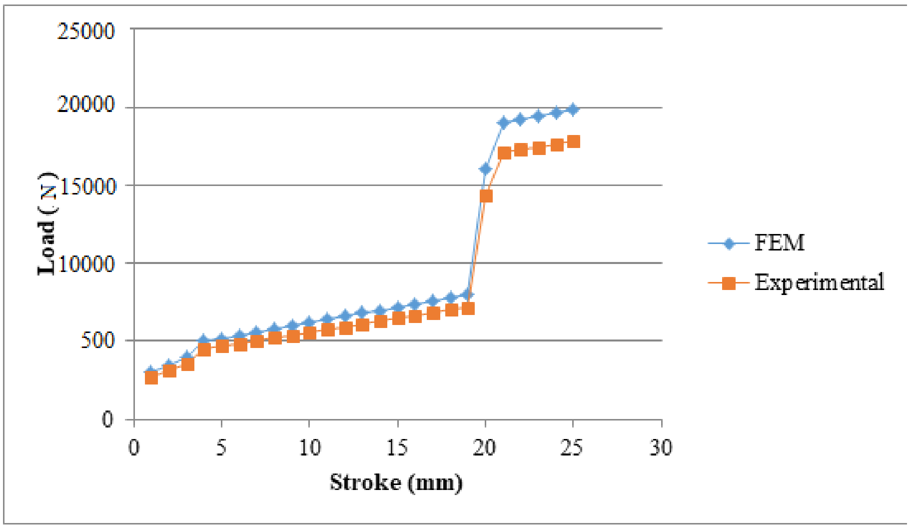

Fig. 27 Load Stroke Diagram of Locally Heated 1.4003

The load stroke curves obtained from experimental work and FEA for locally heated 1.4003 specimens are given in Fig. 27. The difference in bending loads between experimental work and Deform^{TM} 2D simulations is because of lubrication (i.e. friction coefficient). The maximum load is lowered from 22500 N (cold bending) to 20000 N in locally heated specimens

IV. CONCLUSIONS

In this paper the locally heated sheet metal bending experiments and simulations were performed for AZ91B and 1.4003 stainless steel. Finite element simulations were carried out using commercial software DEFORM™ 2D to analyze the process. The FE loads are compared with experimental measurements to validate the FE model. The main conclusions of this research are summarized below:

- In this study, formability problem of the workpiece which is difficult to cold bend was overcome successfully by locally heating the bending area of workpiece.
- The FE model and experimental results are in well agreement.
- It was proven that warm forming is adequate for heat workpiece to give a shape for AZ91B (150^{0}C) and 1.4003 (600^{0}C).
- It was observed that thinning on workpiece is directly related with increasing temperature for AZ91B

REFERENCES

[1] Saha, P., Bhanja, A. (2013). Applications of Stainless Steel in Automobile Industry. *Advanced Materials Research.* **794**, 731–740.
[2] Mustafa Kemal, K. (2008). Magnesium and its alloys applications in automotive industry. The International Journal of Advanced Manufacturing Technology. 39, 851–865.
[3] Lee, E., Hwang, J., Lee, W., Yang, Y., Yang, W. (2014) A local heating method by near-infrared rays for forming of non-quenchable advanced high-strength steels. Journal of Materials Processing Technology. 214, 784–793.
[4] Hino, R., Yoshida, F., Nagaishi, N., Naka, T. (2008).Incremental Sheet Forming With Local Heating for Lightweight Hard-To-Form Material. International Journal of Modern Physics B. 22, 6082–6087.
[5] Kim, S., Lee, Y., (2014). Comparative study on failure prediction in warm forming processes of Mg alloy sheet by the FEM and ductile fracture criteria Metallurgical and Materials Transactions B. 45, 445–453.
[6] Tokita, Y., Nakagaito, T., Tamai, Y., T, Urabe. (2017). Stretch Formability of High Strength Steel Sheets in Warm Forming. Journal of Materials Processing Technology. 246, 77–84.
[7] Ebrahimi, G., Maldar, A., Monajati, H., Haghshenas, M. (2012). Hot deformation behavior of AZ91 magnesium alloy in temperature ranging from 350°C to 425°C. Transactions of Nonferrous Metals Society of China. 22, 2066–2071.
[8] Al-Zubaydi, A., Zhilyaev, A., Wang, S., Reed, P. (2015). Superplastic behaviour of AZ91 magnesium alloy processed by high-pressure torsion. Materials Science and Engineering. 637, 1–11.
[9] Anttila S., Hannu-Pekka H. 2013. Structural Applications of Ferritic Stainless Steels. Luxembourg: RFCS Publications.
[10] Kvačkaj T, Tiža J, Bacsó J, (2014). Cockcroft-Latham Ductile Fracture Criteria for Non Ferrous Materials. Mater Sci Forum.; doi:10.4028/www.scientific.net/MSF, 782, 373.